PROCEEDINGS OF SCIENCE

Kaon-kaon scattering at maximal isospin from $N_f = 2+1+1$ twisted mass lattice QCD

C. Helmes*, **C. Jost, B. Knippschild, B. Kostrzewa, L. Liu, C. Urbach, M. Werner**
University of Bonn
E-mail: helmes@hiskp.uni-bonn.de

We present results for the interaction of two kaons at maximal isospin. The calculation is based on 2+1+1 flavour gauge configurations generated by the ETM Collaboration (ETMC) featuring pion masses ranging from about 230 MeV to 450 MeV at three values of the lattice spacing. The elastic scattering length $a_0^{I=1}$ is calculated at several values of the bare strange quark and light quark masses. We find $M_K a_0 = -0.397(11)(^{+0}_{-8})$ as the result of a chiral and continuum extrapolation to the physical point. This number is compared to other lattice results.

34th annual International Symposium on Lattice Field Theory
24-30 July 2016
University of Southampton, UK

*Speaker.

PoS(LATTICE2016)135

1. Introduction

We investigated the scattering of 2 K^+-mesons in the maximum isospin channel of $I_3 = 1$. Due to $SU(3)$-symmetry breaking by the – compared to the light quark – heavy strange quark, χ-PT often suffers from sizeable corrections. Lattice QCD offers a non-perturbative way to access this interaction and helps in understanding the dynamics of the underlying strong interaction at low energies. We focus on the elastic scattering length of this system which has not been determined experimentally. The analysis of the K^+-K^+-system proceeds very similarly to the one of π-π-scattering at $I_3 = 2$ detailed in ref. [1]. Our study is the first to take into account three values of the lattice spacing.

2. Elastic Scattering in Lüscher's formalism

The scattering length a_0 for the scattering of two mesons is defined by the low energy limit

$$\lim_{q\to 0} q\cot\delta_0(q) = -\frac{1}{a_0}\,, \tag{2.1}$$

where q is the momentum transfer in the center of mass frame and δ_0 the phaseshift of the outgoing wave function. In a series of papers, [4, 5], Lüscher related the scattering length to the energy shift δE of a system of two particles [5] in a finite volume. This energy shift is the deviation of the total energy of the interacting two particle system, E_{KK}, from its expected value in the absence of the interaction between the two particles, $2E_K$. For the case of two K^+-mesons at maximal isospin in the center of mass frame it reads:

$$\begin{aligned}\delta E_{KK}^{I=1} = E_{KK} - 2E_K = -\frac{4\pi a_0}{M_K L^3}\left[1 + c_1\frac{a_0}{L} + c_2\left(\frac{a_0}{L}\right)^2\right] + O(L^{-6})\,,\\ c_1 = -2.9837297, \quad c_2 = 6.375183\,,\end{aligned} \tag{2.2}$$

with the spatial lattice extent L and the kaon mass M_K, where the kaons are at rest.

3. Lattice Action and Operators

We work with Wilson twisted mass Lattice QCD (tmLQCD) at maximal twist introduced in ref. [6]. This guarantees automatic $\mathcal{O}(a)$ improvement of all physical quantities of interest as shown in ref. [7]. The gauge configurations have 2+1+1 dynamical quark flavours and were generated by the ETMC. Their input parameters and the number of evaluated configurations are stated in tab. 1. In total 3 different lattice spacings in the range from 0.619 fm to 0.885 fm and a pion mass range from 230 MeV to 450 MeV build a sound basis for continuum and chiral extrapolations. In this analysis we use twisted mass light valence quarks at maximal twist and Osterwalder-Seiler (OS) strange valence quarks on a Wilson twisted mass fermion-sea. This mixed action approach enables tuning of the valence strange quark mass to its physical value without having to regenerate gauge configurations. The cost of this is introducing small unitarity breaking effects. The Dirac operator for the light sector (used as valence and sea Dirac operator) reads:

$$D_\ell = D_W + m_0 + i\mu_\ell\gamma_5\tau^3\,, \tag{3.1}$$

ensemble	β	$a\mu_\ell$	$a\mu_\sigma$	$a\mu_\delta$	$(L/a)^3 \times T/a$	N_{conf}
*A*30.32	1.90	0.0030	0.150	0.190	$32^3 \times 64$	280
*A*40.24	1.90	0.0040	0.150	0.190	$24^3 \times 48$	404
*A*40.32	1.90	0.0040	0.150	0.190	$32^3 \times 64$	250
*A*60.24	1.90	0.0060	0.150	0.190	$24^3 \times 48$	314
*A*80.24	1.90	0.0080	0.150	0.190	$24^3 \times 48$	306
*A*100.24	1.90	0.0100	0.150	0.190	$24^3 \times 48$	312
*B*35.32	1.95	0.0035	0.135	0.170	$32^3 \times 64$	250
*B*55.32	1.95	0.0055	0.135	0.170	$32^3 \times 64$	311
*B*85.24	1.95	0.0085	0.135	0.170	$32^3 \times 64$	296
*D*30.48	2.10	0.0030	0.120	0.1385	$48^3 \times 96$	369
*D*45.32*sc*	2.10	0.0045	0.0937	0.1077	$32^3 \times 64$	301

Table 1: The gauge ensembles used in this study. The labelling of the ensembles follows the notation in Ref. [8]. In addition to the relevant input parameters we give the lattice volume and the number of evaluated configurations, N_{conf}.

with the Wilson Dirac operator D_W and the Pauli matrices τ^i, $i = 1,2,3$ acting in flavour space. The parameter μ_ℓ denotes the twisted mass $\pm\mu_\ell$ for the spinor χ_ℓ on which it acts ($\chi_\ell = (u,d)^T$). The spinors χ_ℓ ($\bar{\chi}_\ell$) are connected to their physical counterparts, ψ_ℓ ($\bar{\psi}_\ell$), via a chiral rotation,

$$\bar{\psi}_\ell = \bar{\chi}_\ell \exp\left(i\gamma_5\tau_3\frac{\omega}{2}\right), \quad \psi_\ell = \exp\left(i\gamma_5\tau_3\frac{\omega}{2}\right)\chi_\ell, \tag{3.2}$$

around the twist angle ω. Working at maximal twist means $\omega = \pi/2$. For the OS strange valence quarks we use the operator:

$$D_s = D_W + m_0 + i\mu_s\gamma_5. \tag{3.3}$$

Further details of the formulation of the OS action can be found in ref. [9]. The gauge configurations have been generated with the Iwasaki gauge action of ref. [10]. The ensembles cover 11 values of $a\mu_l$ at 3 different lattice spacings a. We calculated strange quark propagators for 3 different strange quark mass parameters $a\mu_s$ per lattice spacing. Tab. 2 states the corresponding values of $a\mu_s$ for every β. The one and two particle operators, in the physical basis denoted by $K(t)$ and $\mathcal{O}_{KK}(t)$,

$$K(t) = \sum_{\vec{x}} \bar{\psi}_s(\vec{x},t)\gamma_5\psi_u(\vec{x},t), \quad \mathcal{O}_{KK}(t) = K(t)K(t),$$

respectively, lead to the correlation functions of the single kaon $C_K(t)$ and the two kaon system $C_{KK}(t)$. They are defined as follows:

$$C_K(t) = \langle K(t)K^\dagger(0)\rangle, \quad C_{KK}(t) = \langle \mathcal{O}_{KK}(t)\mathcal{O}^\dagger_{KK}(0)\rangle.$$

We extract the ground state energy of each correlation function at times large enough such that excited states have decayed sufficiently. Because we work at zero total momentum this approach yields the lattice kaon mass M_K from C_K and the total energy E_{KK} of the K^+-K^+-system from C_{KK}. Unfortunately, the spectral decomposition of C_{KK} gets distorted by terms constant in Euclidean time, preventing the naive extraction of E_{KK}, as detailed in ref. [11]. Following ref. [11] we use a

β	1.90	1.95	2.10
$a\mu_s$	0.0185	0.0160	0.013
	0.0225	0.0186	0.015
	0.0246	0.0210	0.018
a [fm]	0.0885(36)	0.0815(30)	0.0619(18)

Table 2: Values of the bare strange quark mass $a\mu_s$ used for the three β-values and values of the lattice spacing a

ratio of correlation functions

$$R(t+a/2) = \frac{C_{KK}(t) - C_{KK}(t+a)}{C_K^2(t) - C_K^2(t+a)}, \tag{3.4}$$

which can be shown to behave, for large Euclidean times t, like

$$R(t+a/2) \propto A_R \left(\cosh\left(\delta E_{KK} t'\right) + \sinh\left(\delta E_{KK} t'\right) \coth\left(2M_K t'\right)\right), \quad t' = t + \frac{a}{2} - \frac{T}{2}. \tag{3.5}$$

Here T is the total time extent of the lattice. δE_{KK} is obtained by fitting eq. 3.5 to the lattice data of eq. 3.4. We determine a_0 by inserting M_K, L and δE_{KK} into eq. 2.2 and solving for a_0. We apply quark field smearing in a Laplacian-Heaviside (LapH) manner to our quark fields, as proposed in ref. [12], and calculate all-to-all propagators. To reduce the computational costs we combine the LapH method with a stochastic approach (sLapH) as suggested in ref. [13], resulting in 5 (3) random vectors per light (strange) quark perambulator used in the computation. Diluting the random vectors further reduces the stochastic noise. A more detailed description of the sLapH method can be found in reference [1] and references therein.

4. Analysis Strategies

The bare quark mass parameters $a\mu_l$ and $a\mu_s$ are related to their physical counterparts via the renormalisation constant Z_P: $m_f = \mu_s/Z_P$. To work at the physical strange quark mass value we need to specify how to set m_s in our calculation. Setting the strange quark mass in different ways serves as a consistency check.

Method A consists of fixing $a\mu_s$ to the value that reproduces the physical value of the difference

$$\Delta^2 = r_0^2(M_K^2 - M_\pi^2/2) \tag{4.1}$$

on each ensemble. The lattice scale is set using the Sommer Parameter $r_0 = 0.474(14)$ fm and the values for the lattice spacing determined in ref. [14]. Tab. 2 states the values employed for each lattice spacing.

Method B uses the experimental squared kaon mass to fix the strange quark mass via a fit to data for the squared kaon mass as a function of the light and strange quark masses

$$(r_0 M_K)^2 = \bar{P}_0(r_0 m_l + r_0 m_s)\left[1 + \bar{P}_1 r_0 m_l + \bar{P}_2 \left(\frac{a}{r_0}\right)^2\right] K_{M_K^2}^{FSE}, \tag{4.2}$$

which includes lattice artifacts of $\mathcal{O}(a^2)$ [14]. After the fit the continuum values of $(r_0 M_K)^2$ and $r_0 m_l$ from ref. [14] are used to determine the continuum value of $r_0 m_s$.

With the values of $M_K a_0$ interpolated to the strange quark mass of Method A or B we extrapolate the data for $M_K a_0$ in m_l and a to the point of m_l^{phys} determined in ref. [14] and the continuum. In leading order chiral perturbation theory $M_K a_0$ depends linearly on m_l. Because of automatic $\mathcal{O}(a)$-improvement we only have to consider discretisation effects of $\mathcal{O}(a^2)$. In the continuum and the limit $\mu_l \to 0$, we have a residual value of $M_K a_0$, stemming from the non-zero strange quark mass value, giving rise to the parameter P_2 in eq. 4.3. Therefore, we fit the function

$$M_K a_0 = P_0 (r_0 M_\pi)^2 + P_1 \left(\frac{a}{r_0}\right)^2 + P_2 \tag{4.3}$$

to our data at the physical strange quark mass.

5. Results

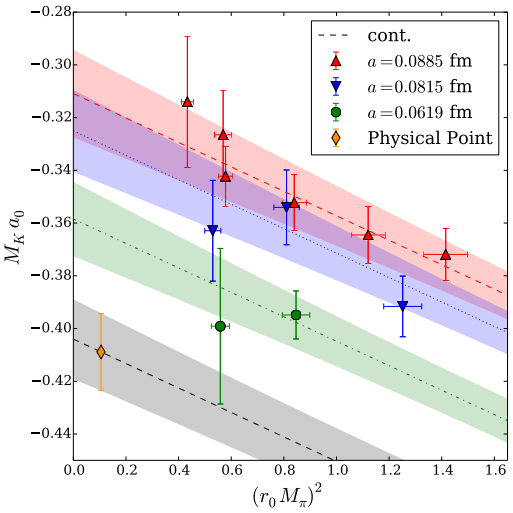

1.a: Chiral and continuum extrapolation of $M_K a_0$ with m_s fixed via Δ^2

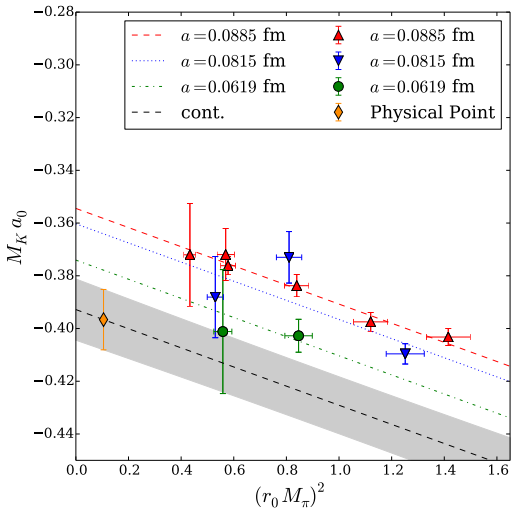

1.b: Same as fig. 1.a, but with m_s fixed via M_K^{exp}. Error bands suppressed for visibility

The fit results for the methods A and B are displayed in fig. 1.a and fig. 1.b, respectively. We show the m_s-interpolated data of $M_K a_0$ as a function of $(r_0 M_\pi^2)$ and the lattice spacing (red, blue and green for rising β). In addition, the fitted functions from eq. 4.3 are shown for each value of the lattice spacing. The continuum extrapolated value of $M_K a_0$, extrapolated to the physical value of M_π^2 together with the continuum version of eq. 4.3 is displayed as well. Despite different discretisation effects, the extrapolated values for $M_K a_0$ calculated with method A and B agree well within errors. They are compiled in table 3. To investigate the different discretisation effects we made a combined fit of the data from methods A and B with common parameters P_0 and P_2 and different parameters P_1 and P_1' for the dependence on the squared lattice spacing a^2. Differences in the discretisation effects should be taken into account by P_1 and P_1'. At the same time the parameters P_0 and P_2 do not change. The extrapolated value of $M_K a_0$ is compatible with the ones from method

	Method A	Method B	A+B combined	p-value weighted
$(M_K a_0)_{\text{phys}}$	$-0.409(15)$	$-0.397(11)$	$-0.405(12)$	$-0.397(11)(^{+0}_{-8})$
χ^2/dof	0.38	0.73	0.65	-
p-value	0.93	0.67	0.86	-

Table 3: Comparison of the results for $M_K a_0$ at the physical point.

A and method B, respectively. The outcome of the combined fit is shown in fig. 2.a and 2.b. The data are the same as shown in fig. 1.a and 1.b. The curves now are results from the fit of eq. 4.3 with the common parameters P_0 and P_2 and the parameters P_1 (fig 2.a) and P_1' (fig 2.b) coming from the different lattice spacing dependence. The fit models both data sets equally well, confirming

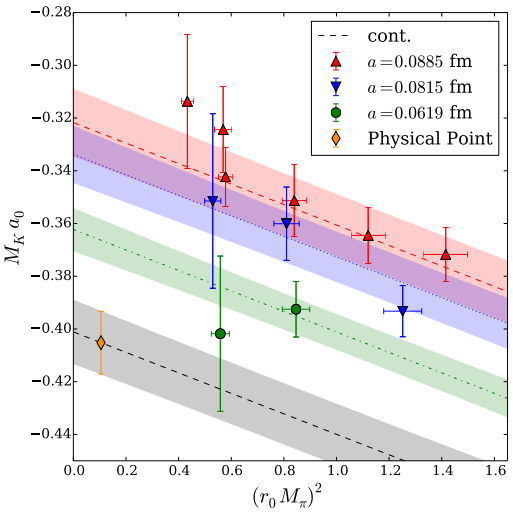

2.a: Combined fit of eq. 4.3 to $M_K a_0$ from method A

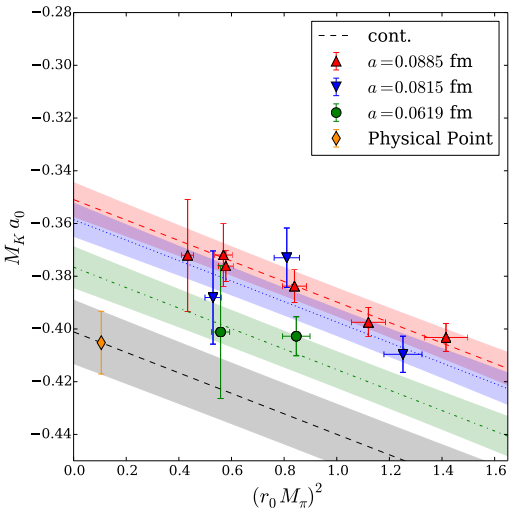

2.b: Same as fig. 2.a with data from method B

that the difference stems from discretisation effects in setting the strange quark mass. To estimate the systematic uncertainty of the Methods A and B we calculate the p-value weighted median of the results from A and B. The results are shown in tab. 3. The 68.54% confidence interval of the combined and weighted distribution of A and B serves as an estimate of the systematic uncertainty.

The NPLQCD collaboration also calculated $M_K a_0$ in ref. [2]. The PACS-CS collaboration undertook an investigation of scattering lengths for systems of two pseudoscalar mesons in ref. [3]. Tab. 4 shows the weighted result for $M_K a_0$ for our work in comparison to the calculations of NPLQCD and PACS-CS. From tab. 4 deviations beyond the statistical level of the three analyses

Collaboration	ETMC(this work)	NPLQCD	PACS-CS
$M_K a_0$	$-0.397(11)(^{+0}_{-8})$	$-0.352(16)$	$-0.310(10)(32)$

Table 4: Comparison of the results of $M_K a_0$ for this work, the work of NPLQCD and the work of PACS-CS. Statistical and systematic uncertainties shown in the first and second parentheses, respectively. For the analysis by NPLQCD stated uncertainty from both uncertainties added in quadrature.

become visible. These differences might be explained with lattice artifacts not taken into account by NPLQCD and PACS-CS at the same level of control.

6. Acknowledgements

We would like to thank the members of the ETMC for the most enjoyable collaboration. The computing time for this project has been made available by the John von Neumann-Institute for Computing (NIC) on the Jureca and Juqueen systems in Jülich. This project was funded by the DFG as a part of the Sino-German CRC110. The open source software packages tmLQCD [15], Boost [16] and SciPy [17] have been used. In addition we employed QUDA [18] for calculating propagators on GPUs.

References

[1] **ETM** Collaboration, C. Helmes *et al.*, JHEP **09**, 109 (2015), arXiv:1506.00408 [hep-lat].

[2] **NPLQCD** Collaboration, S. R. Beane *et al.*, Phys. Rev. **D77**, 094507 (2008), arXiv:0709.1169 [hep-lat].

[3] **PACS-CS** Collaboration, K. Sasaki, N. Ishizuka, M. Oka and T. Yamazaki, Phys.Rev. **D89**, 054502 (2014), arXiv:1311.7226 [hep-lat].

[4] M. Lüscher, Commun.Math.Phys. **104**, 177 (1986).

[5] M. Lüscher, Commun.Math.Phys. **105**, 153 (1986).

[6] **ALPHA** Collaboration, R. Frezzotti, P. A. Grassi, S. Sint and P. Weisz, JHEP **08**, 058 (2001), hep-lat/0101001.

[7] R. Frezzotti and G. C. Rossi, JHEP **08**, 007 (2004), hep-lat/0306014.

[8] **ETM** Collaboration, R. Baron *et al.*, JHEP **06**, 111 (2010), arXiv:1004.5284 [hep-lat].

[9] R. Frezzotti and G. C. Rossi, JHEP **10**, 070 (2004), arXiv:hep-lat/0407002.

[10] Y. Iwasaki, Nucl. Phys. **B258**, 141 (1985).

[11] X. Feng, K. Jansen and D. B. Renner, Phys.Lett. **B684**, 268 (2010), arXiv:0909.3255 [hep-lat].

[12] **Hadron Spectrum** Collaboration, M. Peardon *et al.*, Phys. Rev. **D80**, 054506 (2009), arXiv:0905.2160 [hep-lat].

[13] C. Morningstar *et al.*, Phys.Rev. **D83**, 114505 (2011), arXiv:1104.3870 [hep-lat].

[14] **ETM** Collaboration, N. Carrasco *et al.*, Nucl.Phys. **B887**, 19 (2014), arXiv:1403.4504 [hep-lat].

[15] K. Jansen and C. Urbach, Comput.Phys.Commun. **180**, 2717 (2009), arXiv:0905.3331 [hep-lat].

[16] Boost, *Boost C++ Libraries*, 2003–, http://www.boost.org/.

[17] E. Jones *et al.*, *SciPy: Open source scientific tools for Python*, 2001–, http://www.scipy.org/.

[18] M. A. Clark, R. Babich, K. Barros, R. C. Brower and C. Rebbi, Comput. Phys. Commun. **181**, 1517 (2010), arXiv:0911.3191 [hep-lat].